

Proceeding Paper

Surface Rejuvenation Model for Turbulent Thermophoresis Velocity [†]

Ming-Chi Chiou and Hung-Yih Tsai * 

Department of Vehicle Engineering, National Formosa University, Yunlin 632, Taiwan; achi@gs.nfu.edu.tw

* Correspondence: hungryih@nfu.edu.tw

† Presented at the 3rd IEEE International Conference on Electronic Communications, Internet of Things and Big Data Conference 2023, Taichung, Taiwan, 14–16 April 2023.

Abstract: A mathematical presentation of the surface rejuvenation model is used to relate the mean velocity and temperature distribution to the mean vortex dwell time and approach distance. Coupled with a proper estimate of these modeling parameters, it provides quantitative forecasts of the mean thermophoresis velocity. As expected, the particles obtain inertia along the wall from the eddies in the turbulent core and are trapped in the viscous sublayer where coherent temperature gradients exist in the wall region. Playing an important role in particle transfer, this results in particle transfer along the wall. Particle thermophoresis with small molecule diffusion may be the only mechanism that enhances the particle transfer process in the viscous wall region.

Keywords: surface rejuvenation model; thermophoresis; residence time; approach distance

1. Introduction

The introduction should briefly place the study in a broad context and define the purpose of the work and its significance. A theoretical model of the thermal drift mechanism depends on a description of the thermophoretic velocity of a particle with a temperature gradient. This was first observed for particles that are large compared to the mean free path in the gaseous environment [1]. There was an important parameter affecting thermophoresis, which is defined by the Knudsen number K_n and the mean free path λ of gas molecules and the particle radius r_p .

$$K_n = \frac{\lambda}{r_p} \quad (1)$$

Particle sizes in the mean free paths fall into the continuum, transition, or free molecular regimes, respectively, regardless of the size. Hidy and Brock [2] classified these three regimes according to the values of K_n and suggested that in the slip region, $K_n << 1.0$, in the transition region, $0.25 \leq K_n \leq 10.0$, and in the free molecular environment, $K_n > 10.0$. The mean free path of liquids is orders of magnitude smaller than the mean free path of gases between 0.04 and 0.1 μm under ambient conditions [3].

For large aerosol particles ($K_n << 1.0$), Epstein [1] expressed the thermophoretic force, F_T , in an appropriate form for spherical particles in gas at rest as

$$F_T = -9\pi r_p \frac{\mu^2}{\rho} \left(\frac{K_g}{2K_g + K_p} \right) \frac{\nabla T}{T} \quad (2)$$

where K_p is the particle's thermal conductivity; K_g and ∇T are the thermal conductivity and temperature gradient of gas, respectively. Under the steady-state condition, the thermophoretic force balances the drag force, i.e., $F_T = 6\pi r_p \mu V_t$. Therefore,

$$V_t = -\frac{3}{2} \nu \left(\frac{K_g}{2K_g + K_p} \right) \frac{\nabla T}{T} \quad (3)$$



Citation: Chiou, M.-C.; Tsai, H.-Y. Surface Rejuvenation Model for Turbulent Thermophoresis Velocity. *Eng. Proc.* **2023**, *38*, 42. <https://doi.org/10.3390/engproc2023038042>

Academic Editors: Teen-Hang Meen, Hsin-Hung Lin and Cheng-Fu Yang

Published: 26 June 2023



Copyright: © 2023 by the authors. Licensee MDPI, Basel, Switzerland. This article is an open access article distributed under the terms and conditions of the Creative Commons Attribution (CC BY) license (<https://creativecommons.org/licenses/by/4.0/>).

In Epstein's calculations, the thermal force for particles of high thermal conductivity is significantly underestimated.

Brock [4] indicated that this arises due to a lack of boundary conditions appropriate for the slip flow and the convective terms. For this reason, the modification of thermophoretic force was considered for the case of inclusion of Knudsen number corrections of the temperature increase at the solid-fluid interface and the isothermal slip. In such a way, the corresponding thermophoretic velocity can be appropriately estimated by

$$V_t = -\frac{3}{2}\nu \frac{\left(\frac{K_g}{K_p} + C_t K_n\right)}{(1+3C_m K_n)(1+2\frac{K_g}{K_p} + C_t K_n)} \frac{\nabla T}{T} \quad (4)$$

Brock [4] chose reasonable ranges for the thermal jump coefficient $C_t = 1.875 \sim 2.48$ and for the hydrodynamic slip coefficient $C_m = 1.00 \sim 1.27$. Equation (4) is induced to Equation (3) when $K_n = 0$. Although an agreement was found in the experimental measurements obtained by Jacobsen and Brock [5], the proposed relationship for V_t failed, while for particles with high thermal conductivity, the influence of the values selected for the slip coefficient was significant. However, the discrepancy between experimental and theoretical results is much less than that obtained by using Epstein's model. Derjaguin and Yalamov [6] argued that in the deviation of Epstein's equation and in Brock's work, there are two questions. The first is that the heat flux in the gas volume is ignored, and the second is that boundary conditions are used to assume that, for most gases before hitting the interface, the distribution of the velocity of gas molecules is the same. They modified the boundary conditions to account for the temperature jump and gave a modified expression:

$$V_t = -\frac{1}{2}\nu \frac{8K_g + K_p + 2C_t K_p K_n}{2K_g + K_p + 2C_t K_p K_n} \frac{\nabla T}{T} \quad (5)$$

Derjaguin et al. [7] experimentally confirmed this modification within the limits of experimental error as compared to both the Epstein and Brock models.

The particle radius of small aerosol particles ($K_n \gg 1.0$) is small for the mean free path of the gas. Thus, in the free molecular environment, the particles do not affect the distribution of gas velocity and the force on the moving particle is directly obtained by calculating the momentum transport per unit of time. Waldmann [8] applied this idea for calculating the diffusional velocity of the particle, i.e., the motion of particles due to existing concentration gradients. Since the thermal conductivity is not significant for smaller particles, the thermal force can result from the net impulse in the direction of the temperature gradient imparted to the particles (Equation (6)).

$$F_T = -\frac{32}{15} r_p^2 \frac{K}{\bar{V}} \nabla T \quad (6)$$

where \bar{V} is the average thermal velocity of gas molecules and $K = \frac{15K_g \mu}{4m}$ is the translational part of thermal conductivity with the molecular mass m of gas. Jacobsen and Brock [5] compared the experiment with the thermophoretic force equation of Waldmann [8] and indicated that the equation of F_T was in error by approximately 5% at $\frac{r_p}{\lambda} = 10$ and 10% at $\frac{r_p}{\lambda} = 5$. The corresponding thermophoretic velocity was given by Waldmann and Schmitl [9] as follows.

$$V_t = -\frac{1}{5(1 + \frac{\pi\alpha}{8})} \frac{K_g}{P} \nabla T \quad (7)$$

where P is gas pressure and α is gas thermal diffusivity. It has been demonstrated that this consideration is valid for Knudsen numbers greater than 10 [10].

Talbot et al. [11] modified the Brock model with an improved thermal slip coefficient, which agrees well with experimental measurements for $K_n \leq 0.1$. They have also compared Zernik's concept with fitting the available experimental data accurately over Knudsen

numbers K_n , $0 \leq \frac{\lambda}{r_p} \leq \infty$. In consequence, they proposed a general equation for the thermophoretic force as

$$F_T = -12\pi r_p \mu v \frac{\left(\frac{K_g}{K_p} + C_t K_n\right)}{(1 + 3C_m K_n)(1 + 2\frac{K_g}{K_p} + 2C_t K_n)} \frac{\nabla T}{T} \quad (8)$$

Correspondingly, an improved expression for the thermophoretic velocity can be written as

$$V_t = -2C_s v \frac{\left(\frac{K_g}{K_p} + C_t K_n\right)}{(1 + 3C_m K_n)(1 + 2\frac{K_g}{K_p} + 2C_t K_n)} \frac{\nabla T}{T} \quad (9)$$

in which the velocity jump coefficient $C_m = 1.146$, the temperature increase coefficient is $C_t = 2.18$, and the thermal creep coefficient is $C_s = 1.147$ [12].

2. Surface Rejuvenation Model

The unsteady viscous sublayer surface regeneration model is based on the assumption that fluid eddies occurring at different times reach the core of the turbulence in different distances from the interface. In unsteady momentum and heat transfer, it is assumed that heat transfer is controlled within the wall region such that a single vortex resides near the wall. Neglecting convection and pressure gradient effects, the unsteady transport process of a fluid with constant properties can be written as a single regeneration cycle as

$$\frac{\partial \varphi}{\partial t} = \Re \frac{\partial^2 \varphi}{\partial y^2} \quad (10)$$

where the transport parameter φ represents the axial mean velocity or temperature and t is the instantaneous contact time of eddy. \Re stands for turbulence inertia, $\Re = v + \varepsilon_t$, and for the heat flux, $\Re = \alpha + \alpha_t$. Since both processes of momentum and heat are governed by the same equation, the eddy thermal conductivity α_t and the eddy viscosity ε_t due to the diffusive action of turbulence are equal. The initial condition and boundary condition are given as

$$\begin{aligned} \varphi &= \gamma(y)[1 - U(y - H)] + \varphi_\infty[U(y - H)]att = 0 \\ \varphi &= \varphi_w at y = 0 \\ \varphi &= \varphi_\infty as y \rightarrow \infty \end{aligned} \quad (11)$$

where $U(y)$ is the unit step function, φ_∞ represents the bulk stream velocity u_∞ and temperature T_∞ , and φ_w is a specified temperature T_w of the wall where $u_w = 0$. H is the approach distance of the instantaneous eddy from the wall or the thickness of the viscous sublayer, and $\gamma(y)$ is the initial profile at the first instant of rejuvenation for $y < H$. The quantities t , H , and $\gamma(y)$ follow the statistical distribution with relevant distribution density function $p_t(t)$, $p_H(H)$, and $p_\gamma(\gamma)$. Therefore, by definition, the mean profile can be written as

$$\bar{\varphi}(y) = \int_0^\infty \int_0^\infty \int_0^\infty p_t(t) p_\gamma(\gamma) p_H(H) d\tau d\gamma dH \quad (12)$$

The differential equation in initial-boundary conditions is converted to a domain prior with each term multiplied by the distribution density function. Danckwerts [13] proposed that the contact time is exponentially distributed as

$$p_t(t) = \frac{1}{\bar{\tau}} e^{-\frac{t}{\bar{\tau}}} dt \quad (13)$$

where $\bar{\tau}$ express the mean residence time between two continuous eddies. Because the predictions for the mean transport properties obtained by the Hanratty [14] model are inherently independent of time distribution, the analogical forms of $p_\gamma(\gamma) = e^{-\gamma/\bar{\gamma}}/\bar{\gamma} d\gamma$

and $p_H(H) = e^{-\bar{H}/H} / \bar{H} dH$ are used in this study. The transformed mean profile becomes

$$\bar{\varphi} - \bar{\gamma}(y)e^{-\frac{y}{\bar{H}}} - \varphi_\infty \left(1 - e^{-\frac{y}{\bar{H}}}\right) = \Re \bar{\tau} \frac{\partial^2 \bar{\varphi}}{\partial y^2} \quad (14)$$

where $\bar{\varphi}$ is the mean profile for $p_\gamma(\gamma)$ and $p_H(H)$.

If the contact time t is replaced by that of the residence time τ , $\bar{\gamma}(y)$ can be calculated by

$$\bar{\gamma}(y) = \int_0^\infty \int_0^\infty \int_0^\infty p_\tau(\tau) p_\gamma(\gamma) p_H(H) d\tau d\gamma dH \quad (15)$$

The contact time t in the Danckwert random distribution and residence time τ is related by $\bar{\gamma}(y) = \bar{\varphi}(y)$. This implies that the mean distribution of the residence time at the first moment is the same as the mean distribution of the residence time average. Equation (14) can then be written as

$$(\bar{\varphi} - \varphi_\infty)(1 - e^{-\frac{y}{\bar{H}}}) = \Re \bar{\tau} \frac{\partial^2 \bar{\varphi}}{\partial y^2} \quad (16)$$

and the corresponding boundary conditions are

$$\begin{aligned} \bar{\varphi} &= \varphi_w a t y = 0 \\ \bar{\varphi} &= \varphi_\infty a t y \rightarrow \infty \end{aligned} \quad (17)$$

Accurate analytical solutions of the turbulent convection integrated surface rejuvenation model are obtained as

$$\frac{\bar{\varphi} - \varphi_\infty}{\varphi_w - \varphi_\infty} = \frac{J_{2\beta}(2\beta e^{-\frac{y}{2\bar{H}}})}{J_{2\beta}(2\beta)} \quad (18)$$

where $\beta = \frac{\bar{H}}{\sqrt{\Re \bar{\tau}}}$.

Talbot's equation is adopted to calculate the mean thermophoretic velocity, \bar{V}_t , of the particles, which is expressed as

$$\bar{V}_t = -k \frac{\nu}{\bar{T}} \frac{\partial \bar{T}}{\partial y} \quad (19)$$

where the thermophoretic coefficient k is a ratio of the Knudsen number and other properties of particles. Then,

$$k = \frac{2C_s C_c \left(\frac{K_p}{K_g} + C_t K_n \right)}{(1 + 3C_m K_n)(1 + 2\frac{K_p}{K_g} + 2C_t K_n)} \quad (20)$$

where C_c is the Cunningham correction factor; k is the thermophoretic coefficient, typically varying from 0.2 to 1.2. The temperature gradient is calculated according to Equation (18), which is the same as the result shown in Ref. [15] for the mean temperature distribution in turbulent convective heat transfer, that is,

$$\frac{\bar{T}(y) - T_\infty}{T_w - T_\infty} = \frac{J_{2\theta}(2\theta e^{-\frac{y}{2\bar{H}}})}{J_{2\theta}(2\theta)} \quad (21)$$

where $\theta = \frac{\bar{H}}{\sqrt{\alpha \bar{\tau}}}$. Thus, the distribution of the mean thermophoretic velocity on the wall is obtained by

$$\bar{V}_t = \frac{k\nu}{\sqrt{\alpha \bar{\tau}}} \left(\frac{e^{-(\frac{1}{2\bar{H}})y} J_{2\theta-1}(2\theta e^{-(\frac{1}{2\bar{H}})y}) - J_{2\theta}(2\theta e^{-(\frac{1}{2\bar{H}})y})}{\frac{T_\infty}{T_w - T_\infty} J_{2\theta}(2\theta) + J_{2\theta}(2\theta e^{-(\frac{1}{2\bar{H}})y})} \right) \quad (22)$$

In the wall area, the expression of the average velocity distribution is taken from Equation (19) as follows.

$$\bar{u}(y) = u_\infty \left(1 - \frac{J_{2v} (2v e^{-(\frac{1}{2H})y})}{J_{2v} (2v)} \right) \quad (23)$$

where $v = \frac{\bar{H}}{\sqrt{v\tau}}$. $\bar{\tau}$ is assumed to represent the mean residence time throughout sublayer development. According to the local mean friction velocity, the mean residence time is expressed as u_* from the definition of the wall shear stress $\bar{\sigma}_0 = \rho u_*^2 = \mu \frac{\partial \bar{u}}{\partial y} \Big|_{y=0}$. As a result, the mean residence time is calculated in respect to the commonly used dimensionless quantities by

$$\bar{\tau}^+ = \sqrt{\frac{2}{f}} \left(\frac{J_{2v^+-1} (2v^+) - J_{2v^+} (2v^+)}{J_{2v^+} (2v^+)} \right) \quad (24)$$

where $\bar{\tau}^+ = u_* \sqrt{\frac{\bar{\tau}}{v}}$, $v^+ = \frac{\bar{H}^+}{\bar{\tau}^+}$, and $\bar{H}^+ = \frac{\bar{H}u_*}{v}$. The friction factor f is required and is accurately calculated as $f = 0.07725 \left[\log \left(\frac{Re}{\bar{\tau}} \right) \right]^{-2}$ for the flow by turbulence in smooth tubes [16]. Following this, the dimensionless distribution of the mean thermophoretic velocity on the wall is obtained by

$$\bar{V}_t^+ = \frac{\bar{V}_t}{u_*} = \frac{kPr^{\frac{1}{2}}}{\bar{\tau}^+} \left(\frac{e^{-(\frac{1}{2\bar{H}^+})y^+} J_{2\vartheta^+-1} (2\vartheta^+ e^{-(\frac{1}{2\bar{H}^+})y^+}) - J_{2\vartheta^+} (2\vartheta^+ e^{-(\frac{1}{2\bar{H}^+})y^+})}{\frac{T_\infty}{T_w - T_\infty} J_{2\vartheta^+} (2\vartheta^+) + J_{2\vartheta^+} (2\vartheta^+ e^{-(\frac{1}{2\bar{H}^+})y^+})} \right). \quad (25)$$

where $\vartheta^+ = Pr^{\frac{1}{2}} (\frac{\bar{H}^+}{\bar{\tau}^+})$ and $y^+ = \frac{yu_*}{v}$.

The Bessel function $J_n(x)$ is defined as

$$J_n(x) = \frac{1}{\pi} \int_0^\pi \cos(xs \sin \theta - n\theta) d\theta \quad (26)$$

The function is based on the Sookne's code [17]. The order of the Bessel function must be a positive integer with a backward recursive procedure and strict error control. The relationship between the two passed parameters is defined as

$$\vartheta^+ = Pr^{\frac{1}{2}} v^+ \quad (27)$$

The numerical predictions of thermophoretic velocity distribution are restricted to the positive integers $Pr^{\frac{1}{2}}$ because the orders of the Bessel function v and ϑ of Equations (24) and (25) must be positive integers and n .

3. Results and Discussions

The radial resolute of the fluctuation velocity near the wall region is used to build a viscous sublayer randomly. The analysis result of momentum transfer shows a relationship between the mean residence time $\bar{\tau}^+$ of the mean wall shear stress and the mean velocity profile. A sequence of $\bar{\tau}^+$ and distance \bar{H}^+ is depicted in Figures 1 and 2. Relative to the Reynolds number and dimensionless pipe diameter, the sequence was calculated by

$$d^+ = Re \sqrt{\frac{f}{2}} \quad (28)$$

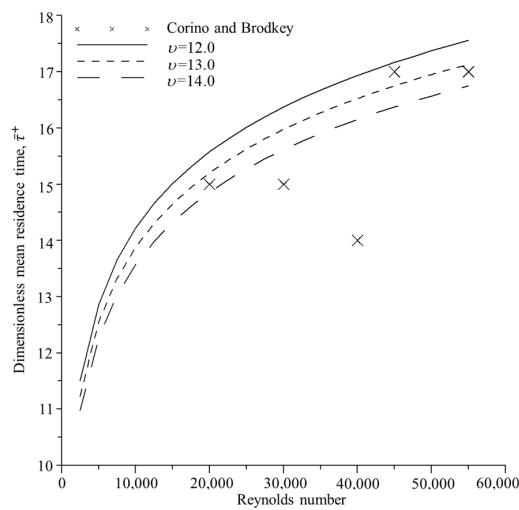


Figure 1. Dimensionless mean residence time with Reynolds number.

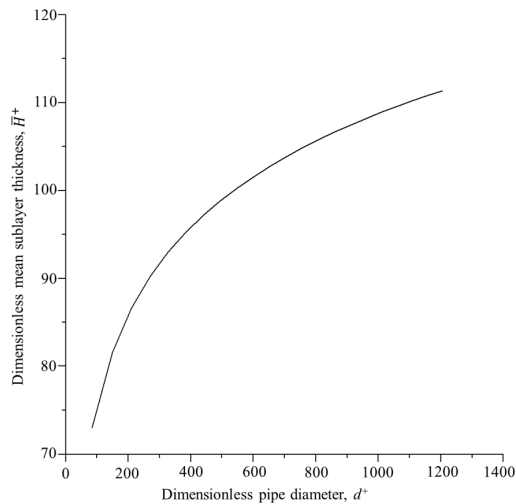


Figure 2. Variation of dimensionless mean sublayer thickness with pipe diameter and Reynolds number.

The eddy appears so frequently at lower Reynolds numbers, and the sublayer development is maintained almost at the wall region. Reversely, the sublayer is progressively established from the wall and seems to be evicted out of the wall region. The variable is a dimensionless mean residence time of turbulence, $\bar{\tau}^+$. The result of the sublayer model by Meek and Baer [18] shows that for Reynolds numbers greater than 10^4 , the mean residence time is constant at 18.0. The visual observations of Corino and Brodkey [19] indicated that the dimensionless cycle period of the viscous sublayer is $14 \leq \bar{\tau}^+ \leq 17$ in the smooth tube flow of $2 \times 10^4 < Re < 5.5 \times 10^4$. The surface rejuvenation model calculation shows that the transfer parameter v is around 13.0; its coinciding with the visual observations (Figure 1) seems satisfactory. Therefore, the prediction of thermophoretic velocity distribution relative to Prandtl number and temperature gradient is calculated with $v = 13.0$ and $\bar{\tau}^+ = 17$ for $Re = 5.0 \times 10^4$.

With fixed values of Reynolds numbers and v , a plot of the calculated thermophoretic velocity relative to Prandtl number is shown in Figure 3 for $T_w - T_\infty = \pm 50^\circ\text{C}$. The thermophoretic velocity becomes greatest near the surface by the steep temperature fluctuation since the sublayer oscillations generate wall temperature fluctuations. The velocity is closer to the surface with increasing Prandtl number and diminishes rapidly in the center of the pipe. The amplitude distribution is broad, especially at low Prandtl numbers, and is

sharper at higher Prandtl numbers. A discrepancy in slope near the edge of the sublayer indicates an enhancing coupling of the thermal and turbulent mechanisms or appears due to the semi-infinite boundary condition.

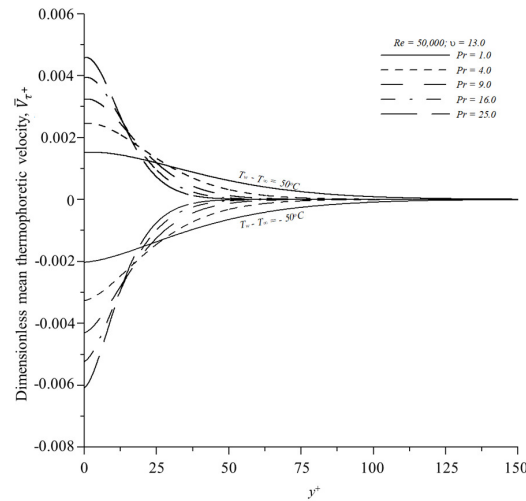


Figure 3. Dimensionless mean thermophoretic velocity distribution with various Prandtl numbers.

If particles are suspended in turbulent flow, turbulence governs the particle transport in the core, which becomes steadily weak when approaching the wall. When the eddy impaction induced by turbulence in the outer boundary layer is acting alone, the particles tend to gather in the viscous sublayer. Coherent temperature gradients are observed along the wall, playing a critical role in particle transport. Figure 4 demonstrates the intensity of the thermophoretic mechanism and indicates a pronounced increase in the thermophoretic velocity with increasing temperature difference, $T_w - T_\infty$. The difference widens at the surface where the thermal gradient is greatest. As expected, thermophoresis of particles with the diffusion of small molecules may be the only mechanism that increases particle transfer near the viscid wall. If thermal fluctuations are higher in the area near the wall, the actual transfer rate is expected to be higher. Changing the temperature gradient in the cooling section significantly affects thermophoretic deposition. When heated, reverse thermophoresis moves particles away from the wall, while the transport by turbulence makes particles move towards the wall. As these two effects interact, particles gather in certain areas close to the wall.

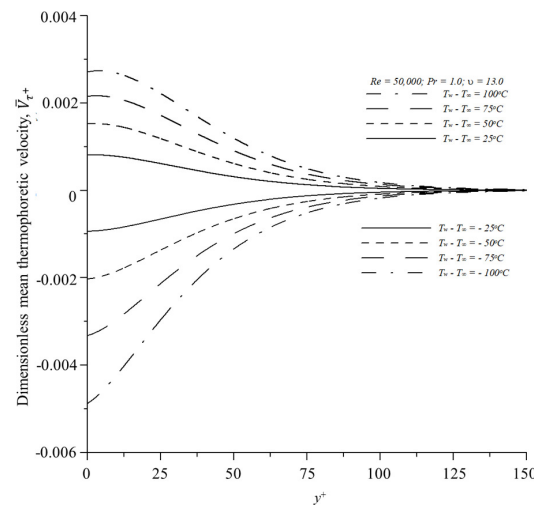


Figure 4. Dimensionless mean thermophoretic velocity distribution with various temperature difference.

Author Contributions: Conceptualization, M.-C.C. and H.-Y.T.; methodology, M.-C.C.; software, M.-C.C.; validation, M.-C.C.; data curation, M.-C.C.; writing—original draft preparation, H.-Y.T.; writing—review and editing, M.-C.C. and H.-Y.T.; supervision, M.-C.C.; project administration, M.-C.C.; All authors have read and agreed to the published version of the manuscript.

Funding: This research received no external funding.

Institutional Review Board Statement: Not applicable.

Informed Consent Statement: Not applicable.

Data Availability Statement: Not applicable.

Conflicts of Interest: The authors declare no conflict of interest.

References

1. Epstein, P.S. Zur theorie des radiometers. *Z. Phys.* **1929**, *54*, 537–563. [[CrossRef](#)]
2. Hidy, G.M.; Brock, J.M. *The Dynamics of Aerocolloidal Systems*; Pergman Press: Oxford, UK, 1970.
3. Whitmore, P.J.; Meisen, A. Estimation of thermo- and diffusionphoretic particle deposition. *Can. J. Chem. Eng.* **1977**, *55*, 279–285. [[CrossRef](#)]
4. Brock, J.R. On the theory of thermal forces acting on aerosol particles. *J. Colloid Sci.* **1962**, *17*, 768–780. [[CrossRef](#)]
5. Jacobsen, S.; Brock, J.R. The thermal force on spherical sodium chloride aerosol. *J. Colloid Sci.* **1965**, *20*, 544–554. [[CrossRef](#)]
6. Derjaguin, B.V.; Yalamov, Y. Theory of thermophoresis of large aerosol particles. *J. Colloid Sci.* **1965**, *20*, 555–570. [[CrossRef](#)]
7. Derjaguin, B.V.; Storozhilova, A.I.; Rabinovich, Y.I. Experimental verification of the theory of thermophoresis of aerosol particles. *J. Colloid Interface Sci.* **1966**, *21*, 35–58. [[CrossRef](#)]
8. Walderman, L. Über die kraft eines inhomogenen gases auf kliene suspendierte. *Z. Nat. A* **1959**, *14*, 588–599.
9. Walderman, L.; Schmitl, K.H. Thermophoresis and diffusiphoresis of aerosol. In *Aerosol Science*; Davies, C.N., Ed.; Academic Press: London, UK, 1966.
10. Tong, T.N.; Bird, G.A. The thermal force in the low density limit. *J. Colloid Interface Sci.* **1971**, *35*, 403–408. [[CrossRef](#)]
11. Talbot, L.; Cheng, R.K.; Schefer, R.W.; Willis, D.R. Thermophoresis of Particles in a Heated Boundary Layer. *J. Fluid Mech.* **1980**, *101*, 737–758. [[CrossRef](#)]
12. Batcheler, G.K.; Shen, C. Thermophoretic deposition of particles in gas flowing over cold surfaces. *J. Colloid Interface Sci.* **1985**, *107*, 21–37. [[CrossRef](#)]
13. Danckwerts, P.V. Significance of liquid-film coefficients in gas absorption. *Ind. Eng. Chem.* **1951**, *43*, 1460–1467. [[CrossRef](#)]
14. Hanratty, T.J. Turbulent exchange of heat and momentum with a boundary. *AIChE J.* **1956**, *2*, 359–362. [[CrossRef](#)]
15. Thomas, L.C.; Ging, P.J.; Chung, B.T.F. The surface rejuvenation model for turbulent convective transport—an exact solution. *Chem. Eng. Sci.* **1975**, *30*, 1239–1242. [[CrossRef](#)]
16. Eck, B. *Technische Stromungslehre*; Springer: New York, NY, USA, 1973.
17. Sookne, D.J. Bessel functions of real argument and integer order. *J. Res. Natl. Bur. Stand. J. Res. B* **1973**, *77*, 125–132. [[CrossRef](#)]
18. Meek, R.I.; Baer, A.D. The periodic viscous sublayer in turbulent flow. *AIChE J.* **1970**, *16*, 841–848. [[CrossRef](#)]
19. Corino, E.R.; Brodkey, R.S. A visual investigation of the wall region on turbulent flow. *J. Fluid Mech.* **1969**, *37*, 1–30. [[CrossRef](#)]

Disclaimer/Publisher's Note: The statements, opinions and data contained in all publications are solely those of the individual author(s) and contributor(s) and not of MDPI and/or the editor(s). MDPI and/or the editor(s) disclaim responsibility for any injury to people or property resulting from any ideas, methods, instructions or products referred to in the content.